Composition of Pluto's Small Satellites: Analysis of New Horizons Spectral Images.

J. C. Cook[1], R. P. Binzel[2], D. P. Cruikshank[3], C. M. Dalle Ore[3,4], A. Earle[2], K. Ennico[3], W. M. Grundy[5], C. Howett[6], D. J. Jennings[7], A. W. Lunsford[7], C. B. Olkin[6], A. H. Parker[6], S. Philippe[8], S. Protopapa[9], D. Reuter[7], B. Schmitt[8], J. A. Stansberry[10], S. A. Stern[6], A. Verbiscer[11], H. A. Weaver[12], L. A. Young[6], the New Horizons Surface Composition Theme Team and the Ralph Instrument Team, [1]Pinhead Institute, Telluride, CO, [2]Massachusetts Institute of Technology, Cambridge, MA, [3]NASA Ames Research Center, Moffat Field, CA, [4]SETI Institute, Mountain View, CA, [5]Lowell Observatory, Flagstaff, AZ, [6]Southwest Research Institute, Boulder, CO, [7]NASA Goddard Space Flight Center, Greenbelt, MD, [8]Institut de Planétologie et Astrophysique de Grenoble, Grenoble, France, [9]University of Maryland, College Park, MD, [10]Space Telescope Science Institute, Baltimore, MD, [11]University of Virginia, Charlottesville, VA, [12]John Hopkins University, Applied Physics Laboratory, Laurel, MD. (jason@pinheadinstitute.org)

Introduction: Orbiting Pluto are 5 satellites: Charon, Styx, Nix, Kerberos and Hydra, in order of increasing distance from Pluto. Charon ($r \sim 600$ km) has been studied from the Earth [1, 2, 3] as well as from *New Horizons* [4, 5]. The remaining satellites are much smaller ($r < 50$ km), irregular in shape [6] and were discovered by Hubble Space Telescope during the construction and cruise phases of *New Horizons* [7, 8, 9]. Learning about these satellites from Earth is difficult. On July 14, 2015, *New Horizons* made its closest approach to the Pluto system. Among its many tasks were spectroscopic observations of Nix, Hydra and Kerberos.

Observations: Using the Ralph [10] instrument, *New Horizons* successfully obtained images and spectra of Pluto's small satellites. Ralph is a dual channel instrument with MVIC (Multi-spectral Visible Imaging Camera), the visible color imager, and LEISA (Linear Etalon Imaging Spectral Array), the near infrared spectrograph. LEISA covers the spectral range 1.25 to 2.50 µm at a resolving power ($\lambda/\Delta\lambda$) of 240, and 2.10 to 2.25 µm at a resolving power of 560. All small satellites, except Styx, were observed with LEISA.

Target	Date, mid-Time (14 July 2015, UT)	Duration (s)	Exp. time (s)	Distance ($\times 10^5$ km)
Kerberos	04:27:16.373	359	0.868	3.94
Hydra	04:46:51.875	458	0.969	3.69
Hydra	07:28:01.876	502	0.854	2.39
Nix	07:56:26.876	340	0.676	1.63
Nix	10:04:04.376	509	0.579	0.60

Methodology: We examine the disk integrated spectrum of each target and the disk resolved spectrum of Nix using Hapke theory. We assume a simple model with an intimate mixture of amorphous H_2O-ice [11], crystalline H_2O-ice [12] in three size ranges, a Triton tholin [13] and a Pluto tholin [14, 15]. We estimate crystallinity and temperature with these data.

Nix: A median LEISA image of Nix (right) and a LORRI + MVIC enhanced color (right, inset) at closest approach. (below, left) The disk integrated spectrum of Nix (black points) is compared to a Hapke model (red curve). We detect several H_2O-ice bands and a deviation at 2.2 µm, likely due to an NH_3-baring material. (below, right) To determine the H_2O-ice phase and temperature, assuming no NH_3, we derive multiple models. The 1.65 µm band in NH_3-H_2O mixtures is suppressed compared to equivalent temperature H_2O-ice. The band also weakens and shifts blueward in crystalline H_2O-ice at higher temperatures [12]. In amorphous H_2O-ice, the same band is weak while other bands extend blueward [11]. We determine a 1-σ temperature upper limit of <60 K, and an 85^{+10}_{-12}% crystalline H_2O-ice fraction.

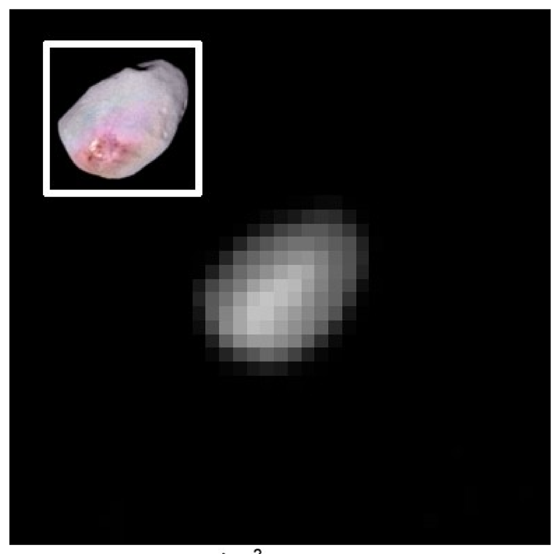

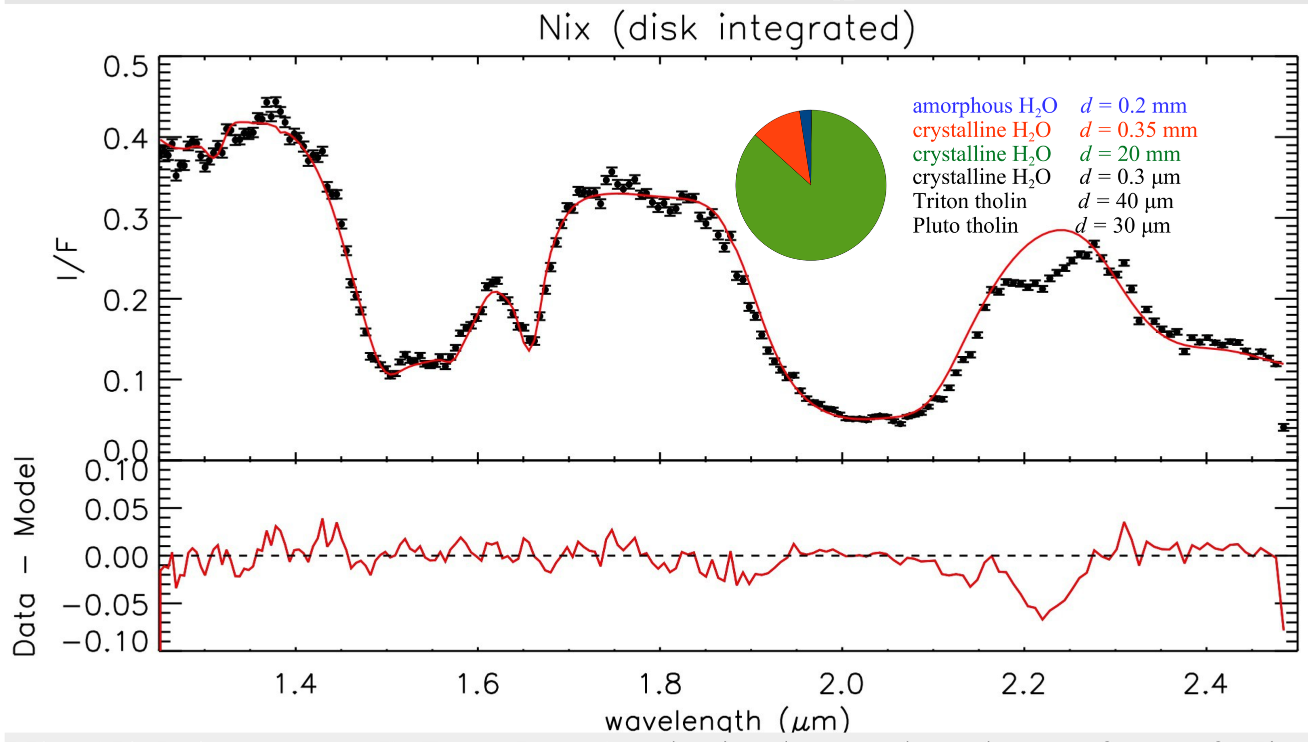

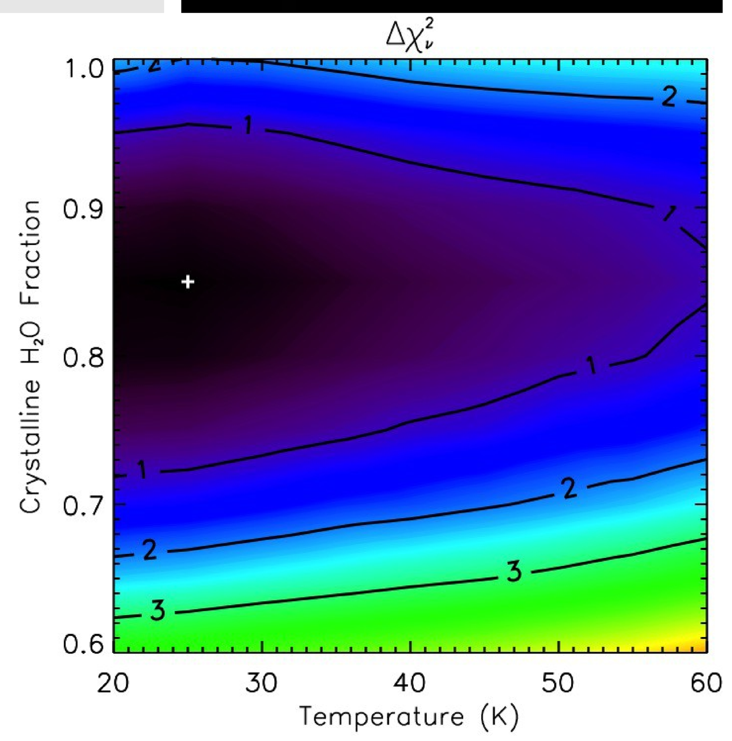

Nix (disk integrated) Results: Analysis shows that the surface of Nix can be best described by a combination of 2.5% amorphous H_2O ice and 97.5% crystalline H_2O. The majority of the crystalline water (89%) is large grained (20 mm), followed by 11% of moderate size (0.35 mm) and a trace fraction of sub-micron size grains. Large grain H_2O likely produces a blue slope. The addition of tholins to the model has a negligible impact on the best-fit.

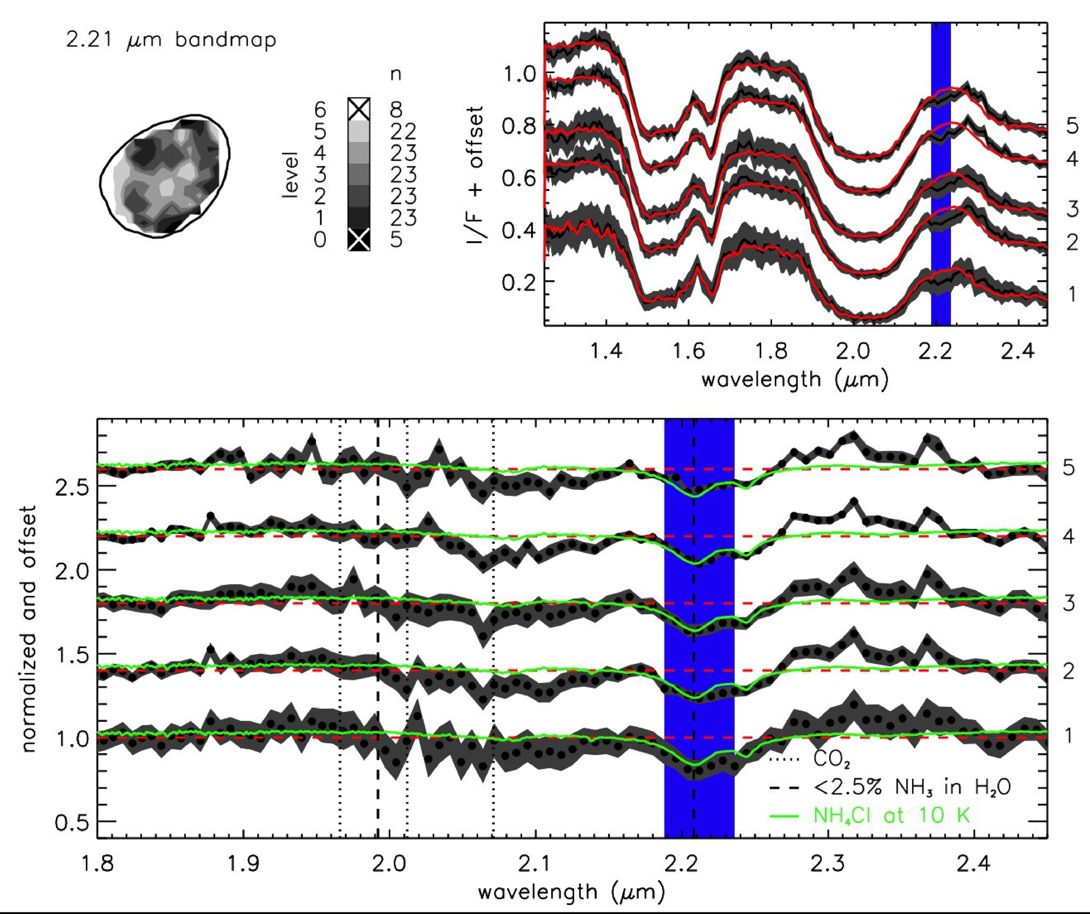

Nix at 2.21 µm: Band depth map of Nix at 2.21 µm (top, far left) with quintile contours, excluding the bottom and top bins. The average spectrum (black lines, top near left) from levels 1 (deepest 2.21 µm band) through 5 (shallowest 2.21 µm band), 3-σ errors (grey) and average Hapke model (red). Band depth is measured by dividing each spectrum by its best-fit Hapke model and integrating over the wavelength range in blue. A detailed look at the normalized spectra (black points, bottom left) are shown from 1.80 to 2.45 µm with 1-σ errors (grey). We clearly detect a band centered at 2.21 µm, and possibly a weaker absorption band around ~2.25 µm. No absorption is evident around 1.99 µm, as would be the case for NH_3•H_2O or NH_3-H_2O-ice mixtures. The observations are compared to NH_4Cl (green, 16) at the same scale for each spectrum.

Hydra: A median LEISA image of Hydra (right) and a LORRI (right, inset) at closest approach. The spectrum (below) of Hydra (black points) is a weighted average of the two LEISA observations. A Hapke model (red curve) is compared to the data. The spectrum clearly shows crystalline H_2O-ice absorption bands at 1.5, 1.65, and 2.0 µm. The residual (data – model) shows a mismatch between the data and model at 2.2 µm similar to that seen on Nix and likely due to an NH_3-baring material (below, right) We examine the average spectrum while varying the crystalline/amorphous H_2O-ice fraction and ice temperature. Because of Hydra's lower signal-to-noise compared to Nix, we determine less significant upper limits on temperature, < 120 K, and crystalline fraction >30%.

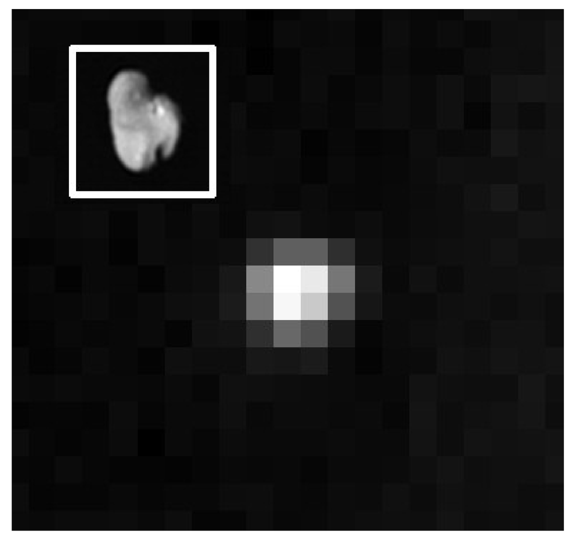

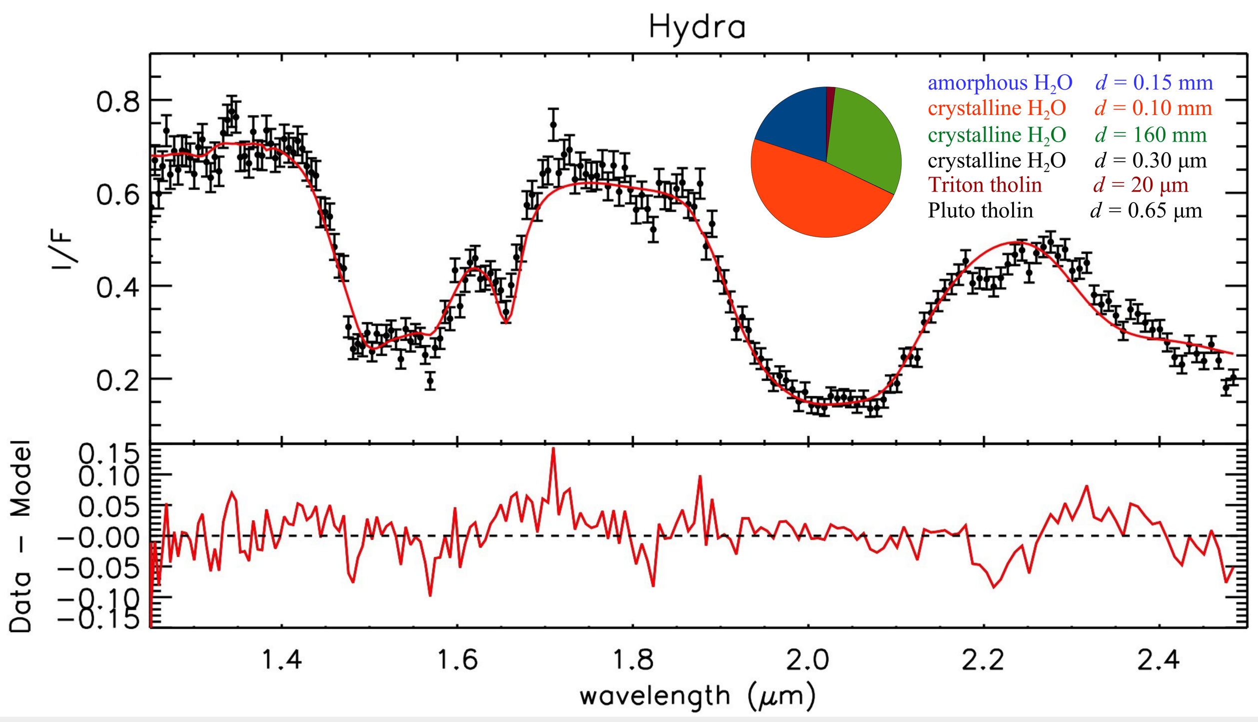

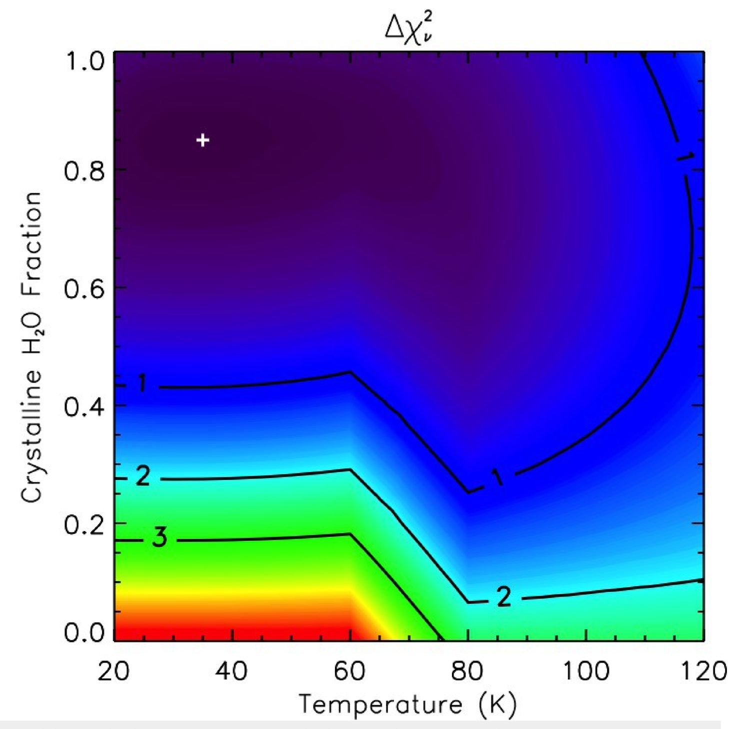

Hydra Results: Analysis shows that the surface of Hydra can be best described by a combination of 20% amorphous H_2O-ice, 10 times more than on Nix, 78% crystalline H_2O-ice and 2% Triton tholins. The majority of the crystalline water (62%) is moderate grained (0.10 mm), followed by 38% of large grained (160 mm) and a trace fraction of sub-micron size grains (0.30 µm). Large grain H_2O likely produces a blue slope.

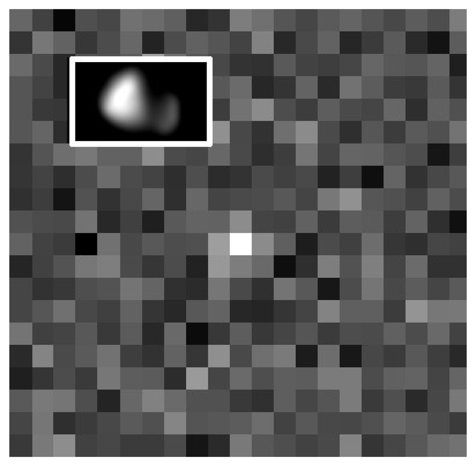

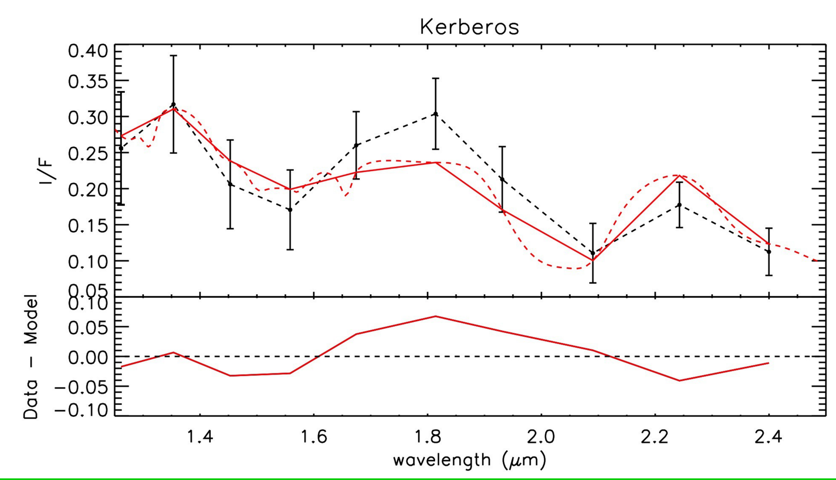

Kerberos: A LEISA (far left) and LORRI (far left, inset) image of Kerberos at closest approach. The spectrum (near left) of Kerberos (black points) has been resampled down to 10 points to increase signal-to-noise. Two bands appear in the spectrum roughly at 1.5 and 2.0 µm. A Hapke model (red solid line) containing only H_2O-ice best matches the data. A model spectrum at the native LEISA sampling is shown as the red dashed line. The residual (data – model) is shown below the spectrum. We cannot determine crystallinity, nor detect NH_3 with these data.

NH_3 in the Solar System: The detection of NH_3-bearing materials suggest that NH_3 may be prevalent in the outer solar system. Below, we show several examples from published papers (Tethys, Verbiscer et al., 2008; Enceladus, Verbiscer et al. 2006; Orcus, Carry et al., 2011; Miranda, Bauer et al., 2002; Ariel, Cartwright et al., 2015; Haumea and Hi'iaka, Barkume et al. 2006), this work and Charon from *New Horizons* [4, 5].

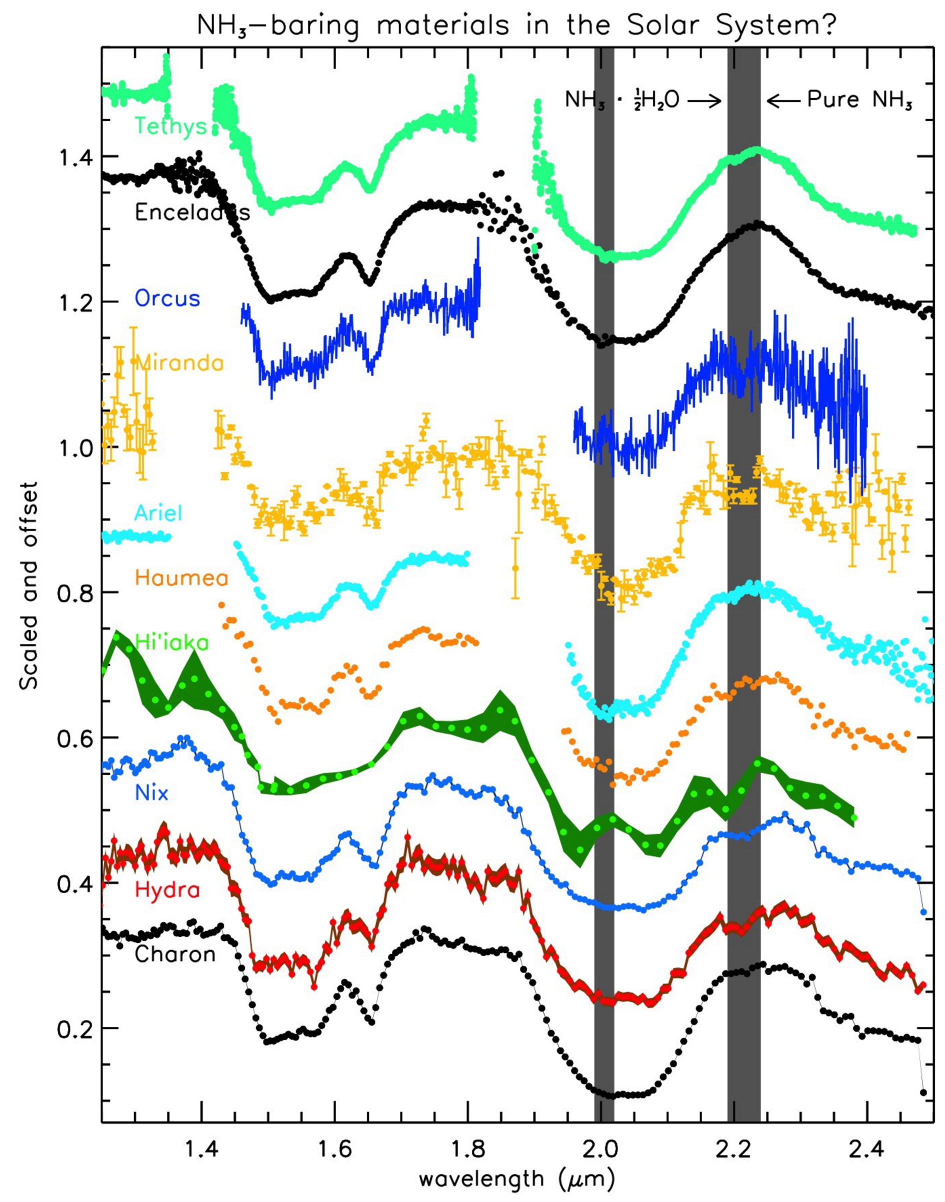

Discussion & Conclusion: This work reports on the composition of Kerberos, Hydra and Nix. These observations show H_2O-ice is present on all three. The greater signal-to-noise of the Nix and Hydra spectra show that the H_2O-ice is in the crystalline phase via the 1.65 µm band. We also find an absorption band at 2.21 µm. This band shows no strong variation in band depth across Nix. This band is likely due to an NH_3-enriched material, such as those identified on Ceres [17], or a mixture with NH_3-H_2O-ice.

References: [1] Buie, M. W., et al., 2000, Icarus, **148**, 324. [2] Sicardy, B., et al., 2006, Nature, **439**, 52. [3] Cook, J. C., et al., 2007, ApJ, **663**, 1406. [4] Dalle Ore, C. M., et al., 2017, Icarus, *submitted*. [5] Cook, J. C., et al., 2017, LPSC, **48**, 2236. [6] Weaver, H. A., et al, 2016, Science, **35**, aae0030. [7] Weaver, H. A., et al., 2006, Nature, **439**, 943. [8] Showalter, M. R., et al., 2011, IAU Circ. 9221. [9] Showalter, M. R., et al., 2012, IAU Circ. 9253. [10] Reuter, D. C., et al., 2008, Space Sci. Rev. **140**, 129. [11] Mastrapa, R. M., et al., 2008, Icarus, **197**, 307. [12] Grundy, W. M., et al., 1998, J. Geophys. Rev. **103**, 25809. [13] Khare, B. N., et al., 1994, Bull. AAS, **26**, 1176. [14] Materese, C. K., et al., 2015, ApJ, **812**, 150. [15] Cruikshank, D. P., et al., 2016, LPSC, **47**, 1700. [16] Moore, M. H et al., 2007, Icarus, **190**, 260. [17] de Sanctis, M. C., et al., 2015, Nature, **528**, 241.